PHYSICAL REVIEW E VOLUME 60, NUMBER 5 NOVEMBER 1999

Ultraresolution in optical imaging using spatiotemporal scanning

Guy Indebetouw and Prapong Klysubun
Department of Physics, Virginia Tech, Blacksburg, Virginia 24061-0435
(Received 7 January 1999; revised manuscript received 8 June 1999)

Spatial information exceeding the passband of an imaging system can be captured by using the optics to generate a spatiotemporal multiple beam interference pattern that is scanned over the object, rather than using it to image the object directly. The modulation of the higher temporal harmonics of the signal resulting from collecting the scattered light represents a mapping in the time domain of higher spatial harmonics of the data. Upon reconstruction, the additional temporal degrees of freedom are mapped back in the spatial domain where they represent spatial frequencies exceeding the passband of the optics. The spatial resolution is thus not limited by the spatial passband, but rather by the temporal bandwidth of the detection system. Due to hardware limitations, experimental demonstration is provided only for a one-dimensional scan of Ronchi gratings with 50 and 200 lines per inch. [S1063-651X(99)51011-8]

PACS number(s): 42.40.Kw, 07.60.Ly, 42.30.Va, 87.64.Rr

Overcoming the spatial resolution limit of imaging systems has been a long-standing quest, and is still actively pursued today. When the imaging system itself cannot be improved directly, super resolving methods have been developed, either to extend its capability, or to compensate for its limitations by data manipulation. The term super resolution, however, has been used in such diverse contexts, that there is some confusion in its definition. In this rapid communication, the following terminology is adopted. Super resolution (which will not be discussed here) is reserved to describe the extension of spatial resolution beyond the half wavelength limit of far-field imaging. Ultraresolution is used to describe the capture or the reconstruction of spatial information that cannot be directly transmitted by the pass band of the optical system. The method described in this letter belongs to this class. Finally, enhancement (also not discussed here) is used to describe the manipulation of the data by numerical algorithms in order to optimize its representation in some defined sense.

Methods addressing the problem of ultraresolution may be grouped into two classes. The first includes the methods based on data inversion [1], and methods exploiting analytical continuation or extrapolation [2]. These methods usually require the solution of nontrivial inverse problems, and in the presence of noise, result in very little gain unless the information is limited to a few degrees of freedom [1]. The methods based on the design of super resolving pupils belong to the same class, and are subject to the same limitations, since the design of these pupils is also an ill-posed inverse problem. Super resolving pupils can be realized as a physical element of the imaging system [3], or can be emulated through post processing [4,5]. The second class of ultraresolution methods include schemes in which the degrees of freedom of the data are rearranged to be compatible with the limited passband of the imaging system [6,7]. This usually requires an additional variable that is used as a coding parameter. Schemes using polarization, wavelength, and time or temporal frequency as coding parameters have been proposed. For example, in spatialtemporal encoding [8], the spatial spectrum is sectioned in parts that can be accommodated individually by the passband of the system, and moving gratings are used to simultaneously encode each section with a different temporal frequency, and to superpose the sections spatially before transmission by the limited system. In these coding schemes, the degrees of freedom of the data are rearranged to match the imaging system, keeping their total number constant [7].

The method described in this Rapid Communication, is different from all of those mentioned. Rather than using the imaging system to transmit spatial information directly, it is used to generate a temporally modulated spatial pattern that is scanned over the object to be imaged. A spatially integrating (nonimaging) detector collects the scattered radiation behind the object. The pattern is generated by a multiple beam interferometer, and thus contains a number of spatial harmonics. With a temporal modulation of the path length of the interferometer, the higher spatial harmonics of the pattern are tagged by the higher temporal harmonics of the modulation signal, which act as multiple temporal carriers. Upon scanning the object spatially, the modulation of a higher temporal harmonic of the detected signal is thus a mapping in the time domain of the corresponding higher spatial harmonic of the spatial data. In this method, time is not merely used as a discreet coding parameter, as in previously proposed coding methods, but is rather used as an additional dimension that extends the phase space of the signal. Upon reconstruction, the additional temporal degrees of freedom are mapped back into the spatial domain where they represent spatial frequencies exceeding the pass band of the optics used to generate the scanning pattern. Consequently, the spatial resolution of this imaging system is not limited by the spatial bandwidth of the optics, but rather by the temporal bandwidth of the detection system.

To demonstrate the idea, a scanning Fabry-Perot étalon was used to generate a scanning pattern containing multiple spatiotemporal harmonics. As will be shown, the multiple beam interference pattern consists of a superposition of spherical waves with curvature radii integer fractions of the focal length f_1 of the first spatial harmonic of the pattern, and temporal frequency shifts integer multiples of the Doppler shift ($\Omega = 4\pi V/\lambda$) resulting from scanning the Fabry-Perot resonance at a rate V (λ is the wavelength). Since the

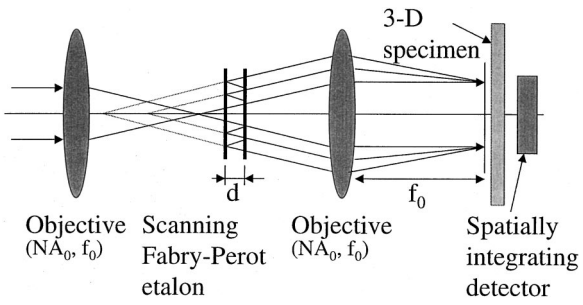

FIG. 1. Sketch of the experimental setup. With objectives with focal length f_0, and a Fabry-Perot with mirror spacing d, a multiple beam, spatiotemporal pattern with focal lengths integer multiples of $f_1 = f_0^2/2d$ is generated and scanned over the object.

radii of curvature of the waves interfering on the object depend on its axial position, not only is the transverse location of an object scatterer encoded in the location, in the time domain, of the signal that it generates, but also its axial location is encoded as well in the shape of that signal. The shape of the signal corresponding to a chosen axial location can be selectively recognized upon digital reconstruction of the data. Thus, the method reconstructs three-dimensional information, and belongs to the class of holographic imaging [9]. The Fabry-Perot scanning makes it possible to record simultaneously a number of holograms at several temporal frequencies $m\Omega$. Assuming that the Nyquist criterion is satisfied, the mth harmonic signal, demodulated at the carrier frequency $m\Omega$, results in an mth harmonic hologram where each object scatterer is encoded with a spherical wave having the fixed size of the scanning pattern, but a radius of curvature f_1/m. The numerical aperture of this encoding wave is thus m times the numerical aperture of the hologram at the fundamental frequency, resulting in an m fold improvement of the transverse resolution, and an m^2 fold improvement of the axial resolution.

The reconstruction of the mth harmonic hologram is done by digital correlation of the holographic data with a spherical wave of radius of curvature f_1/m. Equivalently, the mth harmonic hologram can be reconstructed by correlation with the mth harmonic of the hologram of a single point object acquired experimentally. The latter method offers the interesting possibility of cancelling the aberrations of the objectives. Since the aberrations appear identically in both holographic data (the actual object and the point object), they are cancelled out by the correlation process. The higher harmonic images can be used individually, or the images reconstructed from a number of harmonics can be combined with appropriate weights to obtain a gain of resolution comparable to the well known advantage of a multiple beam interferogram over a two-beam interferogram.

A sketch of the setup used for the experimental demonstration is shown in Fig. 1. A point source is created by an objective with numerical aperture NA_0 and focal length f_0. The resulting spherical wave is transmitted through a Fabry-Perot étalon with mirror spacing d, and reflection coefficient R, which forms a series of virtual point images with axial spacing $2d$, and decreasing amplitudes. The waves from these virtual point sources are collected by an identical objective having the same numerical aperture and focal length. Here $NA_0 = \sin\theta$, where θ is the angle with the axis of the steepest ray entering the objective, which is usually limited by an aperture in its back focal plane. The waves transmitted by the second objective interfere to form, near its back focal plane where the object is located, a ring pattern of radius $a \simeq NA_0 \times f_0$. In a transverse plane at a distance z from the back focal plane of the second objective, the intensity distribution of the scanning pattern has the form:

$$I(\mathbf{r},z,t) = (1-R)^2 \sum_{n=0}^{N} R^n \sum_{m=0}^{N} R^{2m} \times \exp\{i(2\pi/\lambda)(\delta_{n+m} - \delta_n)\} \exp(im\Omega t) + \text{c.c.} \tag{1}$$

where cc stands for complex conjugate, δ_j is the optical path length from the jth virtual point source to a point of coordinate $(\mathbf{r},z)$ in object space, and N is the highest order spherical wave transmitted by the second objective. It is straightforward to show that the difference of optical paths from the $(n+m)$th and the nth virtual point sources interfering at the point of coordinate $(\mathbf{r},z)$ is given by

$$\delta_{n+m} - \delta_n = 2md\{1 - (r^2/2f_0^2) - z[(2n+m)d + x_0](r^2/f_0^4)\}, \tag{2}$$

where x_0 is the arbitrary distance between the back focal plane of the first objective and the front focal plane of the second. The sum over n is readily solved as a geometric progression, giving the intensity distribution of the scanning pattern:

$$I(\mathbf{r},z,t) = \sum_{m=0}^{\infty} E_m(\mathbf{r},z) \exp(im\Omega t) + \text{c.c.}, \tag{3}$$

with

$$E_m(\mathbf{r},z) = R^m (1-R)^2 \times \{1 - R^2 \exp[-imz(2\pi r^2/\lambda)/f_1^2]\}^{-1} \times \exp(im4\pi d/\lambda) \exp\{-im(\pi r^2/\lambda) f_1^{-1} \times [1 + (mf_1^{-1} + 2x_0/f_0^2)z]\} \text{circ}(r/a). \tag{4}$$

Here, $\text{circ}(r) = 1$ for $r < 1$, and $= 0$ otherwise, and $r = |\mathbf{r}|$. In deriving Eq. (4), the following expansions were used: $NA_0 = \sin\theta \simeq \theta, \cos\theta \simeq 1 - \theta^2/2$, which are correct within 10% for $NA_0 < 0.8$. For simplicity's sake, the truncated spherical wave approximation was used to represent the interfering waves. This is valid in the paraxial limit, and with large Fresnel numbers [10]. However, this does not represent a limitation of the method. For optical systems with high numerical aperture, the scanning pattern must only be expressed as a superposition of appropriate diffraction waves instead of the parabolic waves used in the present discussion.

The focal length of the mth spatial harmonic of the scanning pattern is $f_m = f_1/m$, and its equivalent numerical aperture is $NA_m = mNA_1$. For the fundamental $(m=1)$ we have $NA_1 \simeq (f_0/f_1)NA_0$, and $f_1 = f_0^2/2d$. Thus, if for example we choose a Fabry-Perot spacing $d = f_0/2$, the image reconstructed from the first harmonic hologram exhibits transverse and axial resolution limits comparable to those of the objec-

tives used to generate the scanning pattern. However, the higher harmonic holograms recorded in the same conditions will reconstruct information that could not have been directly transmitted by these objectives. The following argument may help in the understanding of how spatial frequencies exceeding the pass band of the optics are indeed captured in the higher temporal harmonics of the signal. In Fig. 1, the scanning imaging process start from the left with the generation of the scanning pattern using two objectives, and ends on the right with a spatially integrating detector. The corresponding conventional imaging system would start from the right with a light source at the location of the detector, and would end on the left with a spatially resolving detector capturing the image formed by the objectives (without the Fabry-Perot). If $2d=f_0$, so that the first harmonic image has a spatial cutoff frequency equal to that of the objective ($NA_1/\lambda=NA_0/\lambda$), a grating with a spatial frequency higher than the cutoff, illuminated from the right by a plane wave, for example, is not resolved by the objectives in the conventional imaging mode. In the scanning mode, from left to right, the first harmonic image will also be incapable of resolving that grating. However, a higher harmonic image, with its spatial frequency cutoff mNA_1/λ, can capture and carry that information and thus reconstruct a resolved image of the grating. An experimental verification of this assertion is given below.

The experimental demonstration made use of a Fabry-Perot interferometer with mirror spacing $d=3$ cm and reflection coefficient $R=0.75$, and a pair of objectives with focal length $f_0=16$ cm. The resulting scanning pattern has a first spatial harmonic focal length $f_1\simeq 40$ cm, and a radius $a\simeq 3$ mm, resulting in a first harmonic numerical aperture $NA_1\simeq 7\times 10^{-3}$. The light source was a He-Ne laser (wavelength 633 nm). The large focal length and modest numerical aperture of the objectives used were dictated by geometrical constraints: the size of the Fabry-Perot available for the experiment prevented the use of objectives with focal lengths smaller than $\sim$15 cm, and diameters larger than $\sim$2 cm. Nevertheless, the purpose of the experiment was not to demonstrate the absolute resolution limit achievable with the method, but rather to illustrate the possibility of capturing spatial frequencies exceeding the bandpass of the optics used to generate the scanning pattern in the higher temporal harmonics of the signal. The Fabry-Perot was piezoelectrically driven at a rate of 5 cycles/s by a saw-tooth voltage, resulting in a fundamental modulation frequency of 25 Hz. Due to hardware limitation (only a one-dimensional scanning stage was available), a single line scan at a speed of 0.1 mm/s was recorded. Figure 2 shows the real part of the first three harmonic holograms of a 15 μm pinhole. These were filtered from the temporal spectrum of the signal, around the carrier frequencies 25, 50, and 75 Hz, and with temporal bandwidths 2.5, 5, and 7.5 Hz, respectively. Mapped in the spatial domain, these bandwidths correspond to spatial frequency cutoffs 12.5, 25, and 37.5 mm^{-1}, respectively.

The hologram of the pinhole was used to reconstruct the holographic data of several objects. This was done by digital correlation of the holographic data of the object with that of the point source, using a standard fast Fourier transform routine. First the reconstruction of the point source itself, which represents the point spread function of the system, is shown in Fig. 3 for the first four harmonic signals. The agreement

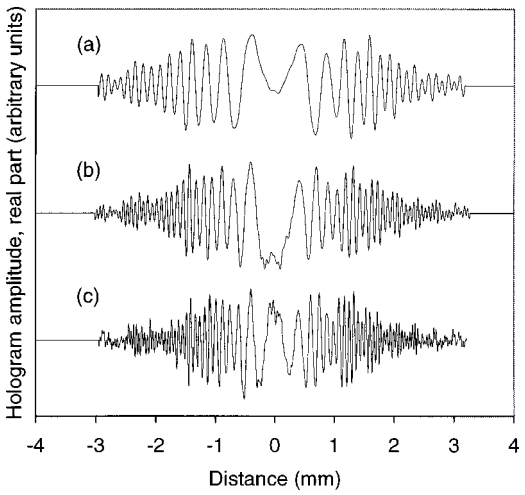

FIG. 2. Holograms of a 15 μm pinhole using the first (a), second (b), and third (c) temporal harmonics of the signal.

with theory, which predicts resolutions of orders 80, 40, 27, and 20 μm, respectively, is convincingly verified. Figure 4 shows the reconstruction of the first three harmonic holograms of a 50 lines per inch Ronchi grating. This result clearly demonstrates how the higher temporal harmonics of the signal, with their additional temporal degrees of freedom, are able to carry higher spatial frequencies of the object. It must be emphasized that with appropriate hardware, allowing the condition $d>f_0/2$ to be satisfied, the scanning pattern that is used in this demonstration could have been generated with an objective of focal length 40 cm, and numerical aperture $\sim 7\times 10^{-3}$, which characterizes the first harmonic of the pattern. The image of the grating formed by this objective would thus have the same resolution as that of the first harmonic image shown in Fig. 4(a). The higher harmonics obviously transmit higher spatial frequencies. An additional demonstration is illustrated in Fig. 5. The object is a 200 lines per inch Ronchi grating. Its spatial frequency is close to the cutoff of the first harmonic ($\sim$250 lines per inch, theoretically). Consequently, it is barely resolved in the first har-

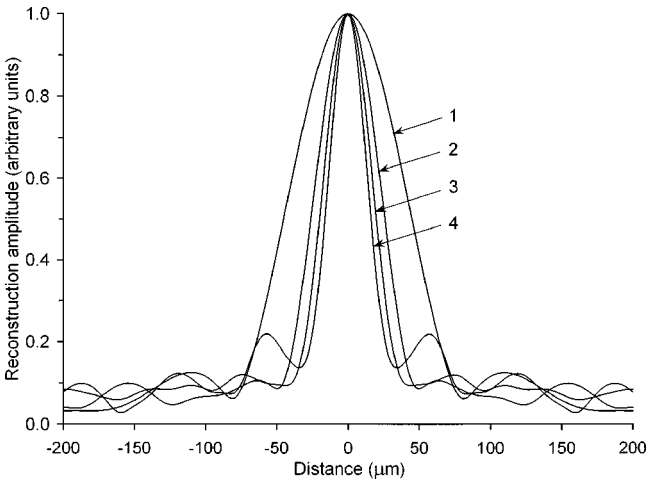

FIG. 3. Reconstructions of the 15 μm pinhole by digital autocorrelation of the first four harmonic holograms (labeled 1 to 4, respectively). This represents the point spread functions of the system for the first four harmonics reconstruction.

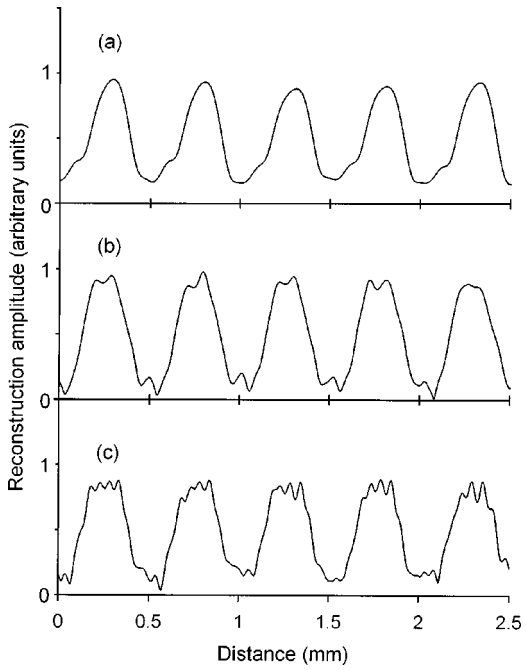

FIG. 4. Reconstruction of a 50 lines per inch Ronchi grating, using the first (a), second (b), and third (c) harmonic of the holographic signal, showing the increased spatial resolution carried by the higher temporal harmonics of the signal.

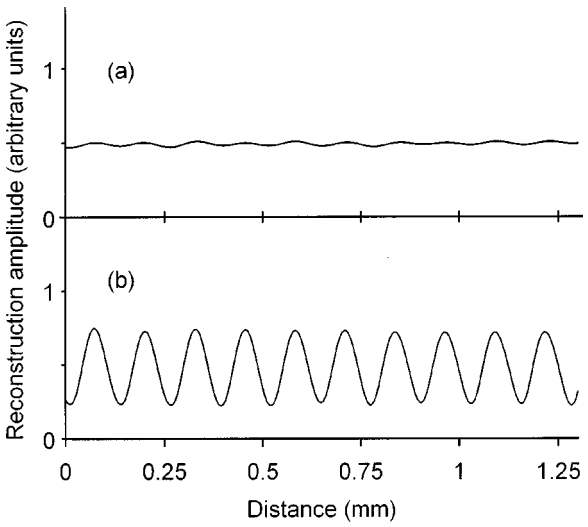

FIG. 5. Reconstruction of a 200 lines per inch Ronchi grating with a spatial frequency close to the first harmonic cutoff. (a), the first harmonic image is barely resolved while (b), the second harmonic image has clearly captured the spatial frequency of the grating.

monic image, as shown in Fig. 5(a). Likewise, this grating would be barely resolved by the objective necessary and sufficient to produce the scanning pattern. In the second harmonic image, however, the grating is well resolved, as shown in Fig. 5(b).

In summary, we have described a method to capture spatial information exceeding the passband of an imaging system. The method employs an interferometric multiple beam scanning imaging scheme in which temporal modulation is used to add time as an additional dimension that carries additional degrees of freedom of the object. The method is remarkably simple to implement. The only difficulty encountered was in synchronizing the Fabry-Perot scan with the modulation of the pattern to maintain their frequencies commensurate. An adequate feedback control should alleviate this difficulty. Upon reconstruction of the data, the additional temporal degrees of freedom carried by the higher temporal harmonics of the signal are mapped back in the spatial domain, where they represent spatial information that can exceed the passband of the optics needed to generate the multiple beam scanning pattern. The resolution of this holographic imaging method is thus not limited by the spatial bandwidth of the optics, but rather by the temporal bandwidth of the detection system, and of course by the number of beams of the scanning pattern. Due to hardware limitation, the method was only demonstrated experimentally for a one-dimensional scanning holographic system with modest resolution. A practical design would make use of high numerical aperture, short focal length objectives, and a compact Fabry-Perot preferably scanned electro-optically.

[1] M. Bertero and C. De Mol, in *Progress in Optics* (Elsevier, Amsterdam, 1996), Vol. 36, p. 129.
[2] G. Torado di Francia, Nuovo Cimento **9**, 426 (1952).
[3] G. Toraldo di Francia, J. Opt. Soc. Am. **45**, 497 (1955).
[4] P. de Santis, F. Gori, G. Guttari, and C. Palma, Opt. Commun. **60**, 13 (1986).
[5] F. Gori, G. Guttari, C. Palma, and M. Santarsiero, Opt. Commun. **67**, 98 (1988).
[6] W. Lukosz, J. Opt. Soc. Am. **56**, 1463 (1966).
[7] W. Lukosz, J. Opt. Soc. Am. **57**, 932 (1967).
[8] P. C. Sun and E. N. Leith, Appl. Opt. **31**, 4857 (1985).
[9] T.-C. Poon, J. Opt. Soc. Am. A **2**, 521 (1985).
[10] W. Wang, A. T. Freiberg, and E. Wolf, J. Opt. Soc. Am. A **12**, 1947 (1995).